

Diffuse X-Ray Scattering from $\text{La}_{2-x}\text{Sr}_x\text{NiO}_4$ and $\text{La}_{2-y}\text{Sr}_y\text{CuO}_4$

E. D. Isaacs,¹ G. Aeppli,¹ P. Zschack,² S-W. Cheong,¹ H. Williams,¹ and D. J. Buttrey³

¹*AT&T Bell Laboratories, 600 Mountain Avenue, Murray Hill, New Jersey 07974*

²*Oak Ridge Institute for Science and Education, Brookhaven National Laboratory, Upton, New York 11973*

³*Department of Chemical Engineering, Colburn Laboratory, University of Delaware, Newark, Delaware 19716*

(Received 29 June 1993)

We use synchrotron x-ray scattering from $\text{La}_{1.8}\text{Sr}_{0.2}\text{NiO}_4$ and $\text{La}_{1.925}\text{Sr}_{0.075}\text{CuO}_4$ to establish a direct relationship between carriers due to Sr doping and strong diffuse scattering. In the nickelate the scattering is peaked at the fourfold symmetric satellite positions $(\pm\delta, \pm\delta, l)$, where the basal-plane coordinate δ varies with the out-of-plane coordinate l of the momentum transfer. A similar scattering pattern is observed in the cuprate, but with smaller values for δ .

PACS numbers: 74.72.Dn, 61.10.-i

Substitution of Sr for La has a dramatic effect on the magnetic properties of the layered transition metal oxides La_2MO_4 . In particular, for $M = \text{Cu}$, as the material becomes metallic and superconducting, incommensurate magnetic fluctuations replace the Néel order of pure La_2CuO_4 [1]. While a similar level of Sr doping induces neither superconductivity nor even metallic behavior in La_2NiO_4 [2], it does destroy Néel order [3], yielding a spin glass with incommensurate correlations [4]. The latter are different from those found in the cuprate in that in the zero frequency limit they are of shorter range, frozen, and characterized by wave vectors along the $[\pm\pi, \pm\pi]$ rather than the $[0, \pm\pi]$ and $[\pm\pi, 0]$ directions in the nearly square MO_2 planes. Furthermore, the incommensurate fluctuations are most likely due to Fermi surface nesting in $\text{La}_{2-x}\text{Sr}_x\text{CuO}_4$, while they should be related to the frozen arrangement of carriers in $\text{La}_{2-x}\text{Sr}_x\text{NiO}_4$. In either case, however, incommensurate charge fluctuations or order which one could associate with the known magnetic correlations have yet to be identified, extensive structural studies of these materials notwithstanding [5,6]. We have therefore used synchrotron x-ray diffuse scattering to search for the atomic displacements which such fluctuations would induce. Our key result is that for both the Cu and Ni compounds doping does lead to diffuse streaks whose integrated intensity is a remarkable 0.5% of that for nearby Bragg peaks [e.g., the (0,0,10) reflection]. These streaks appear as fourfold incommensurate peaks along the $[\pm\pi, \pm\pi]$ directions in the reciprocal space of the MO_2 planes. Apart from the finding of smaller incommensurability, the cuprate displays streaks qualitatively similar to those for the nickelate. Taking advantage of the tunable x-ray energies at the synchrotron, we also demonstrate that the streaks do not arise from displacements of the Sr acceptors. They must therefore be due to the transition metal and oxygen motion derived from the holes which the Sr acceptors contribute.

Recent electron diffraction studies have yielded sharp, commensurate superlattice peaks which were attributed to polaron lattice formation [7]. Unfortunately, unlike x-ray scattering, the electron scattering technique is in-

capable of probing bulk samples and cannot be interpreted quantitatively because of the strong coupling of the charged probe to the sample. We sometimes observe the same sharp, commensurate peaks as in the electron diffraction measurements [8], but they are at least 2 orders of magnitude weaker than the strong diffuse streaks which are reproducible in all samples with the appropriate oxygen annealing.

Our $\text{La}_{1.925}\text{Sr}_{0.075}\text{CuO}_{4\pm z}$ sample was a $7 \times 5 \times 0.3$ mm³ [0,0, l] plate of the type used previously [1]. The $2 \times 2 \times 0.2$ mm³ $\text{La}_{1.8}\text{Sr}_{0.2}\text{NiO}_{4\pm z}$ sample was prepared as described in Ref. [9] with a shiny, cleaved [0,0, l] surface and was annealed just prior to the measurements for 10 h at 850°C in oxygen at 200 bars. At $T = 10$ K, the lattice parameters are $a = 3.840$ Å, $b = 3.839$ Å, and $c = 12.673$ Å, in good agreement with previous determinations for ceramics with the same nominal composition [2]. The dc resistivity in the a - b plane of this sample is approximately $100 \mu\Omega \text{ cm}$ at $T = 300$ K, growing exponentially to $1 \Omega \text{ cm}$ by $T = 100$ K, where, surprisingly, it becomes flat down to at least $T = 2$ K [10]. Finally, the bulk susceptibility becomes hysteretic below 120 K, in agreement with the onset temperature for spin freezing found by Hayden *et al.* for a similar specimen [4].

We collected the x-ray scattering data at the National Synchrotron Light Source on beam lines X14 and X25. The sample was mounted with the [0,0, l] reciprocal lattice vector aligned in the vertical scattering plane of the four-circle diffractometer. The incident energy was tuned to 16.0 keV, 105 eV below the Sr K -absorption edge, to maximize sample volume (absorption length $1/\mu \cong 120 \mu\text{m}$) while avoiding contamination of the signal by Sr K -edge fluorescence. We used an argon or xenon gas filled proportional counter as a detector (~ 3 keV energy resolution at 16 keV) and two pulse-height analyzers to separate the Ni (Cu) K -edge fluorescence at 7.478 keV (8.048 keV) from the signal. The K -edge fluorescence intensity was used to normalize the signal intensity to compensate for sample volume effects. Throughout this paper the data are described using reciprocal lattice units (rlu) in the tetragonal coordinate system (ignoring the small orthorhombic distortion), with the two short axes defined

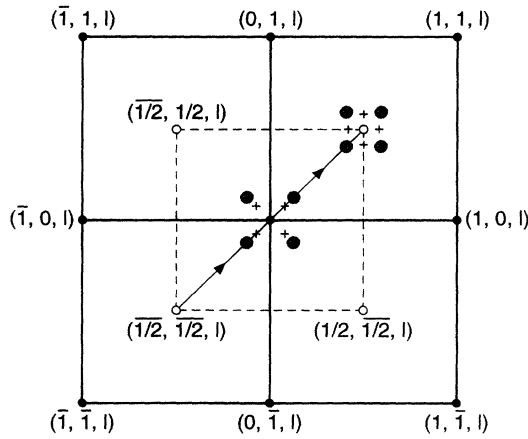


FIG. 1. Reciprocal space for the NiO₂ or CuO₂ planes. The solid line with arrows is a representative $[h, h, 0]$ line scan described in the text. The dashed box indicates the region of the contour plots in Figs. 2(a) and 2(b). Included in this figure are the peak positions of the diffuse scattering in the nickelate (circles) and cuprate (crosses) samples for both x-ray (blue) and neutron scattering (red).

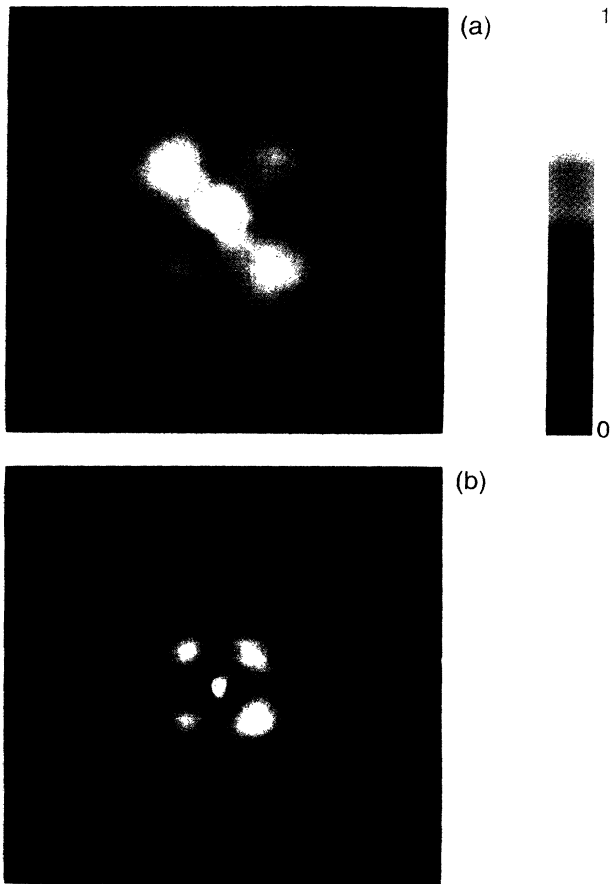


FIG. 2. (a) Contour plot of the $[h, k, 7.6]$ reciprocal lattice plane in La_{1.8}Sr_{0.2}NiO₄ at $T = 300$ K. (b) Contour plot of the $[h, k, 13.6]$ reciprocal lattice plane (equivalent reduced wave vector $\Delta l = 0.4$ rlu) in La_{1.925}Sr_{0.075}CuO₄ at $T = 10$ K.

as the distance between the nearest-neighbor nickel (copper) atoms along the Ni-O (Cu-O) bonds. In this system the $(2\pi, 0)$ and $(0, 2\pi)$ Bragg points correspond to the $[1, 0, l]$ and $[0, 1, l]$ lines.

Figure 1 shows the reciprocal space of the square NiO₂ or CuO₂ planes. When this plane is imbedded in the full three-dimensional reciprocal space of La_{2-x}Sr_xMO₄, the vertices of the grid cross at Bragg points when $h+k+l$ is even, e.g., $(0, 0, 8)$ or $(1, 1, 6)$. In this figure we plot the positions of our diffuse x-ray scattering peaks (blue) taken for the reduced wave vectors $\Delta l = 0.4$ in the nickelate (open circles) and the cuprate (crosses) samples.

Figure 2(a) shows a contour plot of the diffuse scattering intensity in La_{1.8}Sr_{0.2}NiO₄ in the $[h, k, 7.6]$ reciprocal lattice plane at $T = 300$ K. These data have two important features: (a) intense (~ 1500 counts/sec), fourfold

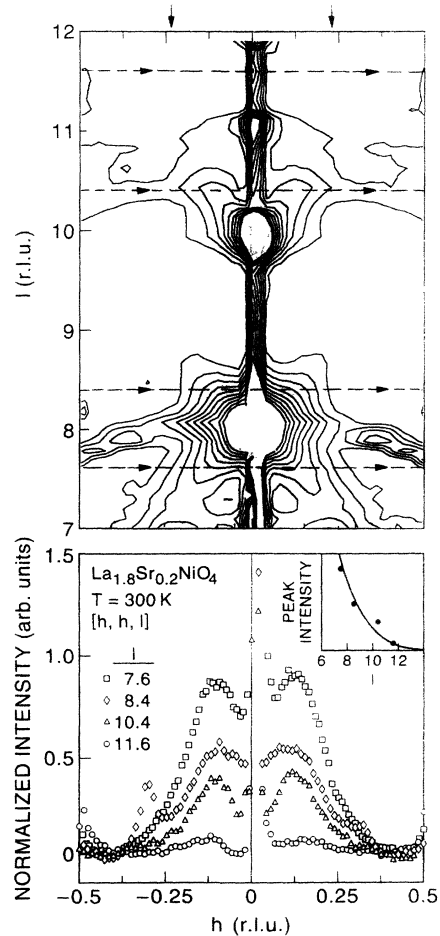


FIG. 3. Upper panel: Contour plot of diffuse scattering intensity in the $[h, h, l]$ plane with $T = 300$ K showing the c^* -axis dependence to the diffuse scattering. The contour lines are spaced at intervals of 0.1 in arbitrary units. The blue bands indicate the peak positions of the streaks which extrapolate to $\delta \cong 0.21$ in the middle of the zone. Lower panel: $[h, h, l]$ line scans from the contour in the upper panel (dashed lines). Inset: integrated intensities of $[h, h, l]$ line scans.

symmetric diffuse scattering peaks and (b) an apparently square background whose sides are parallel to the $[1,1,0]$ and $[-1,1,0]$ directions. The bright spot at $q = (0,0,7.6)$ is a cut through a resolution-limited rod of scattering along $[0,0,l]$ (see Fig. 3). Four Gaussians centered at the positions $(\pm\delta, \pm\delta, l)$, plus four more Gaussians, accounting for the square background, which are centered at $(\pm\delta', 0, l)$ and $(0, \pm\delta', l)$, give a good description of the overall intensity distribution. Our best fit of this function to the 2D mesh yields the values $\delta \cong 0.126 \pm 0.005$ rlu with HWHM of $\xi^{-1} \cong 0.14 \text{ \AA}^{-1}$ and $\delta' = 2\delta \cong 0.272 \pm 0.005$ rlu with a HWHM $\xi^{-1} \cong 0.22 \text{ \AA}^{-1}$. These fitting parameters are remarkable in that if we consider the inner peaks to be the $(2\pi, 0)$ and $(0, 2\pi)$ primary reflections in a square lattice, the outer Gaussian peaks are at approximately the next order [the $(\pm 2\pi, \pm 2\pi)$ square reciprocal lattice points]. Furthermore, the fact that the $(2\pi, 2\pi)$ peak is $\sqrt{2}$ broader than the $(2\pi, 0)$ peaks indicates that the diffuse peaks arise from a strain modulation of the lattice. A similar, but weaker scattering pattern is observed at $T = 10$ K. It is interesting that the symmetry of the diffuse x-ray scattering is identical to that of the 2D incommensurate magnetic scattering observed with neutrons [4]. However, while the x-ray peaks are satellites of the zone center Bragg peaks, the neutron peaks are satellites of the antiferromagnetic Bragg peaks observed [3] in the undoped La_2NiO_4 , i.e., the $(1/2, 1/2, l)$ points.

The diffuse scattering pattern in the $[h, k, 0]$ plane in $\text{La}_{1.925}\text{Sr}_{0.075}\text{CuO}_4$ is strikingly similar to that for the nickelates and is shown in Fig. 2(b) for the $[h, k, 13.6]$ reciprocal lattice plane at $T = 10$ K. This contour plot is at the same reduced wave number, $\Delta l = 0.4$, along c^* as that for the nickelate in Fig. 2(a). While the peaks centered at $(\pm\delta, \pm\delta, l)$ are still quite strong, the square background is more difficult to observe at this lower temperature. A fit of these data by just the inner peaks described in the previous paragraph gives a best fit with $\delta \cong 0.08 \pm 0.005$ rlu with HWHM of $\xi^{-1} \cong 0.07 \text{ \AA}^{-1}$.

Figure 3 shows a contour plot of the diffuse scattering in the $[h, h, l]$ plane for $\text{La}_{1.8}\text{Sr}_{0.2}\text{NiO}_4$ at $T = 300$ K. It is evident that Fig. 2(a) with $l = 7.6$ is a planar cut through fourfold oblique streaks. These streaks carry a remarkably large weight, when integrated over a Brillouin zone (e.g., from $l = 8$ to 10), which we estimate to be 0.5% of the scattering at the nearby Bragg peak [e.g., $(0,0,10)$]. The streaks cross at the Bragg points and reach a maximum extrapolated value of $\delta \cong 0.21$ near the middle of the zone (blue bands). The rod of scattering along the $[0,0,l]$ direction is resolution limited in the $[h, k, 0]$ plane and is most likely associated with stacking faults. The arc that passes through the $(0,0,8)$ reflection is a powder ring. For large momentum transfer the streaks are difficult to see in the contour plot but are evident in the $[h, h, 0]$ line scans taken for four equivalent wave numbers with $\Delta l = 0.4$. The diffuse intensity is peaked at the same position of $\delta \cong 0.11$ for all four scans.

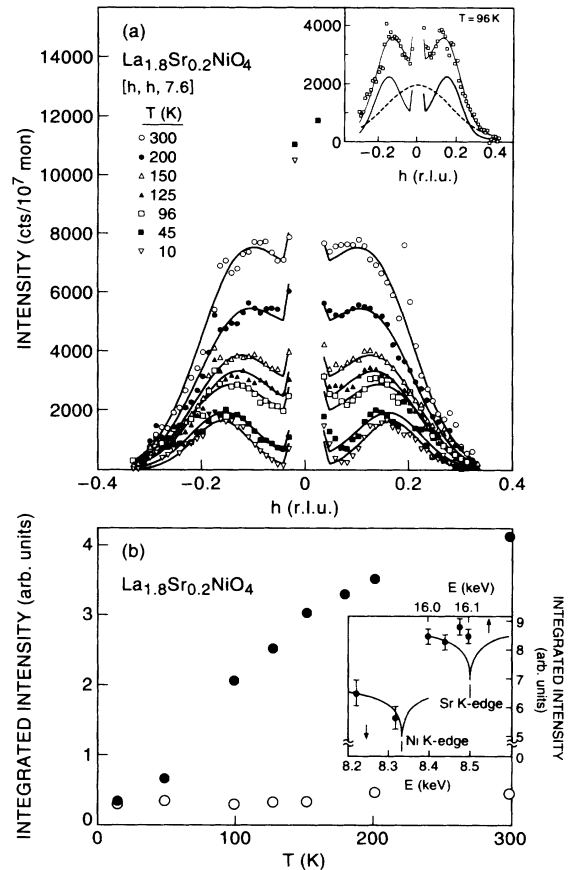


FIG. 4. (a) $[h, h, 7.6]$ line scans for $T = 10, 45, 96.6, 125, 150, 200,$ and 300 K. Inset: Plot of fourfold Gaussian (solid line) and broad single Gaussian components (dashed line) for $T = 96.6$ K. (b) The integrated intensities of the fourfold Gaussian component (open circles) and the broad single Gaussian component (filled circles) from the fits shown in 4(a).

The inset shows the large decrease in integrated intensity with the total momentum transfer, $|\mathbf{Q}|$. From a fit to the data of a Debye-Waller form we obtain a large rms displacement along the c axis for the scattering atoms of $\langle u_s^2 \rangle^{1/2} \cong 0.4 \text{ \AA}$.

In Fig. 4 we plot $[h, h, 7.6]$ line scans repeated for seven temperatures between $T = 10$ and 300 K. A flat background has been subtracted from each of the scans and we ignore the sharp peak at $h = 0$. The scans contain two distinct components which are shown in Fig. 4(b); (i) a broad Gaussian distribution centered on $[0,0,l]$, and (ii) the inner peaks from the fourfold symmetric function described above. Figure 4(b) shows the temperature dependence of the integrals of the components (i) (filled circles) and (ii) (open circles). The first component grows by an order of magnitude between $T = 10$ and 300 K, and might be ascribed to the activation of phonons with a typical frequency of 100 K, considerably below the Debye temperature (see Ref. [11]). The second diffuse component, describing the $(1,0)$ -type

peaks in Fig. 2(a), depends much more weakly on temperature. Thus, it must arise from static atomic displacements [11], or may be due to phonons with a frequency high compared to our measuring temperatures of ~ 30 meV [12]. However, in the latter case the associated phonon amplitudes would be pathologically large.

Finally, we have determined that the diffuse scattering arises from the presence of the doped holes and is not derived from the Sr acceptors. This follows because measurements on an undoped crystal of La_2NiO_4 show no evidence of the diffuse scattering, although depending on the oxygen treatment they did show sharp peaks of the $(1/1, 1/3, l)$ type seen in electron diffraction (Ref. [7]). Furthermore, $[h, h, 7.6]$ line scans were repeated for several incident energies near the Sr K edge (16.105 keV). The inset in Fig. 4(b) shows that the integrated intensity does not vary, in contrast to what is expected for the anomalous corrections at the Sr K edge (solid line). The errors in these data are not statistical but originate from uncertainties in the increasing fluorescence background as the absorption edge is approached. Thus we conclude that, to within experimental error, the diffuse scattering is not derived from the Sr acceptors and so is most likely associated with holes residing in the NiO_2 layers. This idea is consistent with preliminary data (see inset of Fig. 4), which indicate a depression of the intensity near the Ni K edge.

In summary, we have discovered that Sr doping induces strong diffuse x-ray scattering in the layered transition metal oxides $\text{La}_{2-x}\text{Sr}_x(\text{Ni,Cu})\text{O}_4$. In both systems the integrated scattering weight over a Brillouin zone is about 0.5% of the Bragg peaks. The scattering has the same fourfold symmetry about the c^* axis for both materials, but with a smaller extent parallel to the planar directions in the more lightly doped cuprate sample investigated. Anomalous scattering shows that carriers must be liberated from the Sr acceptors, which do not themselves contribute to the diffuse streaks, to yield motions of the transition metal and oxygen ions. The frozen magnetic correlations in the doped, but nonmetallic, nickelate yields a pattern with the same symmetry, i.e., with incommensurate wave vectors δ along $[\pm 2\pi, \pm 2\pi]$ (see Fig. 1). A relationship, which might be based on charged domain walls, between the x-ray and neutron results is plausible given that the magnetic wave vector is one-half of the maximum (extrapolated) x-ray wave vector [13]. Even so, it will be a challenge to reconcile the three-dimensional nature of the x-ray streaks with the two-dimensional incommensurate magnetic scattering. In contrast, for the metallic cuprate, the magnetic and x-ray

scattering appear unrelated, with the magnetic pattern associated with Fermi surface nesting [14], rotated by 45° with respect to the diffuse x-ray pattern. Thus, notwithstanding their very different transport and magnetic properties, the two transition metal oxides share a doping induced tendency for the particular lattice instability discovered in our experiments.

We thank T. T. M. Palstra for sharing his bulk data with us and J. Zaanen and P. Littlewood for many inspiring discussions. We would also like to thank H. Mook, P. Platzman, L. Berman, M. Nelson, and G. Wright for their help. Oak Ridge National Lab beam line X14A is supported in part by DOE Contract No. DE-AC05-84OR21400.

-
- [1] T. R. Thurston *et al.*, Phys. Rev. B **40**, 4585 (1989); S.-W. Cheong *et al.*, Phys. Rev. Lett. **67**, 1791 (1991); T. E. Mason *et al.*, Phys. Rev. Lett. **68**, 1414 (1992).
 - [2] R. J. Cava *et al.*, Phys. Rev. B **43**, 1229 (1991).
 - [3] G. Aeppli and D. J. Buttrey, Phys. Rev. Lett. **61**, 203 (1988); G. H. Lander *et al.*, Phys. Rev. B **40**, 4463 (1989); T. Freltoft *et al.*, Phys. Rev. B **44**, 5046 (1991); J. Rodriguez-Carvajal *et al.*, J. Phys. Condens. Matter **3**, 3215 (1991).
 - [4] S. M. Hayden *et al.*, Phys. Rev. Lett. **68**, 1061 (1992).
 - [5] S. J. L. Billinge and T. Egami, Phys. Rev. B **47**, 14386 (1993); J. D. Axe *et al.*, Phys. Rev. Lett. **62**, 2751 (1989).
 - [6] J. M. Tranquada *et al.*, Phys. Rev. Lett. **70**, 445 (1993).
 - [7] C. H. Chen, S.-W. Cheong, and A. S. Cooper, Phys. Rev. Lett. **71**, 2461 (1993).
 - [8] These commensurate peaks were seen in both the Sr doped and undoped nickelates. We have also seen sharp commensurate peaks in the doped cuprates, however, these fourfold peaks were observed at $(1/3, 0, l)$ and $(0, 1/3, l)$ positions, i.e., rotated by 45° relative to the nickelates. At present, we see no obvious relation between our diffuse scattering peaks and those seen with electron diffraction in Ref. [7].
 - [9] D. J. Buttrey *et al.*, J. Solid State Chem. **54**, 407 (1984).
 - [10] T. T. M. Palstra *et al.* (private communication).
 - [11] X. Jiang *et al.*, Phys. Rev. Lett. **67**, 2167 (1991), and references therein.
 - [12] L. Pintschovius *et al.*, Phys. Rev. B **40**, 2229 (1989).
 - [13] J. Zaanen and O. Gunnarsson, Phys. Rev. B **40**, 7391 (1989); J. Zaanen and P. Littlewood (to be published).
 - [14] P. Littlewood *et al.*, Phys. Rev. B **48**, 487 (1993); P. Bénard *et al.*, Phys. Rev. B **47**, 589 (1993); Q. Si *et al.*, Phys. Rev. B **47**, 9055 (1993); N. Bulut and D. J. Scalapino, Phys. Rev. B **45**, 2371 (1992).

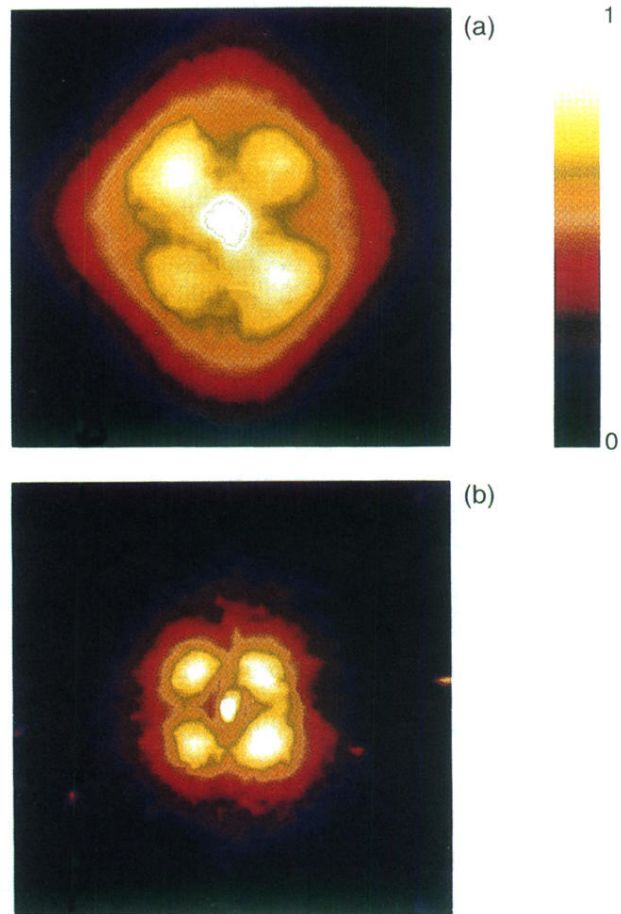


FIG. 2. (a) Contour plot of the $[h, k, 7.6]$ reciprocal lattice plane in $\text{La}_{1.8}\text{Sr}_{0.2}\text{NiO}_4$ at $T = 300$ K. (b) Contour plot of the $[h, k, 13.6]$ reciprocal lattice plane (equivalent reduced wave vector $\Delta_l = 0.4$ rlu) in $\text{La}_{1.925}\text{Sr}_{0.075}\text{CuO}_4$ at $T = 10$ K.

